Sustainable Processes Connect
ISSN: 3079-1421
2026, Article ID. 2026.0028, Cite as: https://doi.org/10.69709/SusProc.2026.188988

SCIFINITI PUBLISHING

Research Article

OPEN ACCESS

Data-Driven Optimization of Plant-Derived Bio-Coagulants for TDS Removal from Paint Wastewater: Comparative RSM and ANN Modeling

Onyekachi Stephen Nnamani✉, **Benson Chinweuba Udeh**✉, **Cyprian Obinna Azinta**✉,*

Department of Chemical Engineering, Enugu State University of Science and Technology, Agbani, Enugu PMB 01660, Nigeria

Article History
Received: April 15, 2026 Accepted: July 22, 2026 Published: August 25, 2026

Abstract
This work investigated and optimized the efficiency of total dissolved solids (TDS) removal from paint wastewater (PWW). Sustainable natural coagulants derived from avocado pear seed (PS) and *Moringa oleifera* seed (MOS) were used to reduce TDS in PWW, with Fourier Transform Infrared spectroscopy and proximate analysis employed to characterize the materials. The results revealed major functional groups, proteins, and polysaccharides known to facilitate the coagulation-flocculation process. Response surface methodology (RSM) with a central composite design was used to determine the optimum combination of bio-coagulant dosage, pH, and settling time, while an Artificial Neural Network (ANN) model, developed from the same experimental data, was applied to better capture the complex, nonlinear relationships among the variables. The ANN model consistently outperformed RSM in prediction accuracy for both bio-coagulants, based on statistical indicators such as R^2, RMSE, and SEP. For PS, ANN achieved $R^2 = 0.9998$, RMSE = 0.12, and SEP = 0.144813, compared with RSM values of $R^2 = 0.990407$, RMSE = 0.86902, and SEP = 1.048711. For MOS, ANN attained $R^2 = 1.0000$, RMSE = 5.3×10^{-5}, and SEP = 6.15×10^{-5}, again exceeding RSM performance ($R^2 = 0.987555$, RMSE = 1.009331, SEP = 1.171387). Under optimized conditions, TDS removal efficiencies reached 93.53% for PS and 97.24% for MOS, and statistical analysis confirmed significant linear, interaction, and quadratic effects of the operational factors. Both PS and MOS thus emerge as promising, greener alternatives to conventional chemical coagulants, with the combined RSM-ANN approach providing a reliable, data-driven framework for predicting TDS removal performance and optimizing operating conditions.

Keywords:
artificial neural network; bio-coagulants; response surface methodology; total dissolved solids removal; paint wastewater; pear seed; *Moringa oleifera* seed

1. Introduction

Releasing untreated paint wastewater (PWW) into receiving water bodies poses serious environmental concerns, because it contains a high concentration of total dissolved solids (TDS), resins, solvents, pigments, and other complex organic and inorganic constituents that degrade water quality and threaten aquatic ecosystems [1]. Conventional treatment methods commonly rely on chemical coagulants such as alum and ferric salts; however, growing concerns over residual metal toxicity, excessive sludge generation, rising operational costs, and environmental sustainability have driven increasing interest in greener treatment alternatives [1–3].

Bio-coagulants extracted from plant materials such as *Moringa oleifera* and avocado pear seeds have attracted considerable attention because of their biodegradability, low toxicity, local availability, and cost effectiveness [3–5]. Their coagulation-flocculation performance is mainly attributed to naturally occurring proteins and polysaccha-

* Corresponding Author:
Cyprian Obinna Azinta, Department of Chemical Engineering, Enugu State University of Science and Technology, Agbani, Enugu PMB 01660, Nigeria, azinta.acom@gmail.com

© 2026 Copyright by the Authors.
Licensed as an open access article using a CC BY 4.0 license.

rides, which promote particle destabilization, charge neutralization, and floc formation [4,5], aligning well with ongoing efforts toward sustainable wastewater treatment and the valorization of agricultural by-products. Despite this promise, treatment efficiency remains highly sensitive to operational parameters, making process optimization essential for practical application.

Coagulation-flocculation and adsorption are among the most widely used technologies for removing dissolved and suspended pollutants from wastewater. Coagulation-flocculation is generally preferred for its rapid destabilization of pollutants, ease of operation, and effectiveness in treating wastewaters with high particulate and colloidal loads [3,5–9], whereas adsorption is known for its strong affinity for residual dissolved pollutants, owing to the active surface sites on adsorbent materials [10–13]. Adsorption systems, however, frequently demand longer contact times, regeneration procedures, and disposal of spent adsorbents [10–12]. Plant-derived bio-coagulants offer an appealing alternative, since they can simultaneously drive coagulation-flocculation and adsorption-assisted removal within a single treatment step [10]—supporting floc formation while removing dissolved contaminants through charge neutralization, particle bridging, and surface contact, and thereby reducing reliance on conventional chemical coagulants in favor of more sustainable wastewater treatment [8,9].

Advanced modeling techniques are increasingly used to investigate process factors and their interactions and to optimize bio-coagulant-based wastewater treatment processes. Response Surface Methodology (RSM) is widely applied for process optimization, since it can examine multiple operating parameters simultaneously and generate predictive polynomial models [14,15]; wastewater treatment systems, however, often display complicated nonlinear behavior that traditional statistical methods may fail to capture adequately [16]. Artificial Neural Networks (ANNs) have therefore attracted growing attention for their ability to learn directly from experimental data and model nonlinear relationships with strong predictive accuracy [16–18]. Recent studies point to the increasing use of machine learning and statistical optimization techniques for sustainable wastewater treatment using various bio-based adsorbents and coagulants derived from agricultural residues [6,8,12,14–24], demonstrating that ANN and RSM can jointly optimize bio-based materials, improve pollutant removal efficiency, and reduce both treatment costs and environmental impact. Meftah et al. [23], for example, applied ANN and RSM to optimize dye removal using activated carbon derived from plant biomass, achieving strong prediction accuracy and process efficiency, while Meftah et al. [12], Zahmatkesh et al. [20], and Ding et al. [22] have each underscored the growing importance of machine learning in driving optimization, advancing sustainable wastewater treatment technologies, and facilitating the scale-up of bio-based materials.

Despite these advances, the comparative performance of RSM and ANN models for predicting TDS removal using locally sourced avocado pear and *Moringa oleifera* seed bio-coagulants remains largely unexplored, particularly for paint wastewater treatment. This work is motivated by the goal of recovering resources from waste and developing sustainable, low-cost, data-driven treatment technologies capable of improving industrial wastewater management. Accordingly, the study is limited to evaluating the performance of avocado pear and *Moringa oleifera* seed bio-coagulants for TDS removal from paint wastewater, assessing the effects of dosage, pH, and settling time on treatment efficiency, and comparing the predictive capabilities of RSM and ANN models. In doing so, it contributes to the growing body of knowledge on sustainable wastewater treatment by offering both process optimization insights and comparative modeling evidence for these bio-coagulants.

2. Materials and Methods

2.1. Equipment, Reagents, and Bio-Coagulant Preparation

The research was conducted using standard laboratory equipment, including a magnetic stirrer, an electronic balance, a graduated cylinder, beakers, a mortar and pestle, a pH meter, an oven, Whatman No. 1 filter paper, and a stopwatch. Avocado pear seeds (PS) and *Moringa oleifera* seeds (MOS) served as the bio-coagulants, alongside paint wastewater (PWW) and distilled water, while the reagents used included sodium hydroxide, hydrochloric acid, ethylenediaminetetraacetic acid (EDTA), and buffer solutions. PS and MOS were prepared separately following the methods described in [4,25]—washing, sun-drying, and grinding to a fine powder—after which the active ingredients were extracted by suspending 5 g of each powdered bio-coagulant in 100 mL of distilled water, stirring the mixture for 15 min at room temperature, and filtering it through Whatman No. 1 filter paper. Fresh bio-coagulant solutions were prepared before each experiment to ensure consistent results.

2.2. Paint Wastewater Sampling

Wastewater from paint production was collected, with permission from Legacy Paints Limited, at the final effluent disposal point of the company's facility in Emene Indus-

2026, Vol. 2, Article ID. 2026.0028
https://doi.org/10.69709/SusProc.2026.188988

trial Layout, Enugu State, Nigeria, during peak production in February 2024. Samples were collected in pre-washed, acid-rinsed polyethylene containers to prevent contamination and preserve their physicochemical properties, stored at 4 °C, and analyzed within 24 h according to the procedure described in [4]. Initial TDS concentration was measured prior to treatment.

2.3. Coagulation-Flocculation (Jar Test) Experiments

TDS removal was evaluated using a six-paddle jar test setup as described by [4]. Paint wastewater samples were rapidly mixed at 100 rpm for 5 min to ensure adequate coagulant dispersion, then mixed slowly at 40 rpm for 25 min to promote floc formation, and then allowed to settle for 55 min. The filtered clear supernatant was then tested for TDS, and removal efficiency was estimated using Equation (1) [4]:

$$\text{TDS removal}(\%) = \frac{C_0 - C_t}{C_0} \times 100 \qquad (1)$$

where C_0 is the initial TDS concentration of the paint wastewater sample and C_t is the final TDS concentration after coagulation-flocculation treatment.

2.4. Bio-Coagulant and Wastewater Characterization

The functional groups in PS and MOS associated with coagulation were identified using Fourier Transform Infrared (FTIR) spectroscopy. TDS, the primary focus of this study, was measured gravimetrically in accordance with standard methods [26], while other wastewater characteristics were noted but not analyzed further in this work.

2.5. Experimental Design and Optimization Using RSM

A Central Composite Design (CCD) within the Response Surface Methodology (RSM) framework was used to optimize TDS removal across three coded factors: dosage (A), pH (B), and settling time (C). A face-centered CCD ($\alpha = 1$) was chosen to avoid extreme axial points [27]. Experimental design, regression analysis, analysis of variance (ANOVA), response surface generation, determination of optimum TDS removal values for both bio-coagulants, and numerical optimization were all performed using Design-Expert software (Version 9.0.1). The resulting design was a three-factor, three-level face-centered central composite design comprising 20 experimental runs (Table 1), each conducted as described in Section 2.3.

2.6. Artificial Neural Network (ANN) Modeling

Artificial Neural Network (ANN) modeling was performed to predict TDS removal efficiency using the MATLAB Neural Network Fitting Tool (nftool, MathWorks Inc., USA), using dosage, pH, and settling time as inputs and TDS removal efficiency as the output. The dataset was randomly split into training (70%), validation (20%), and testing (10%) subsets: the training data established the relationship between process variables and TDS removal efficiency, the validation data assessed model performance during training and guarded against overfitting, and the testing data evaluated the predictive capability of the resulting network. A feed-forward backpropagation neural network comprising an input layer, one hidden layer, and an output layer was developed, with the Levenberg-Marquardt algorithm adopted as the training function for its suitability to nonlinear prediction problems [18,19]. The output layer used a linear transfer function (purelin), while the hidden layer used a tangent sigmoid (tansig) function; the number of hidden neurons was optimized by trial and error to minimize the mean square error (MSE), and the architecture yielding the lowest prediction error was ultimately selected. Predictive performance was then evaluated through regression analysis and the coefficient of determination (R^2), root mean square error (RMSE), and standard error of prediction (SEP) [18–20].

2.7. Comparative Analysis of RSM and ANN

The predictive performance of the RSM and ANN models was compared using Equations (2)–(4) [19,20]:

Root Mean Square Error (RMSE):

$$RMSE = \left(\frac{1}{n}\sum\nolimits_{i=1}^{n}(Y_{pred} - Y_{exp})^2\right)^{\frac{1}{2}} \qquad (2)$$

Coefficient of Determination (R^2):

$$R^2 = 1 - \frac{\sum_1^n (Y_{exp,i} - Y_{pred,i})^2}{\sum_1^n (Y_{exp,i} - Y_{exp,ave})^2} \qquad (3)$$

Standard Error of Prediction (SEP):

$$SEP = \frac{RMSE}{Y_{exp,ave}} \times 100 \qquad (4)$$

where Y_{pred} is the predicted TDS removal, Y_{exp} is the experimental TDS removal, $Y_{exp,ave}$ is the average experimental TDS removal, and n is the number of data points; Y_{pred}, Y_{exp}, and $Y_{exp,ave}$ are all expressed as percentages.

Table 1: Central composite design matrix for TDS removal experiments.

Run	A: Dosage (g)	B: pH	C: Time (min)
1	4	4	40
2	5	6	30
3	5	2	50
4	3	6	30
5	4	4	30
6	4	4	50
7	4	4	40
8	4	4	40
9	5	2	30
10	4	4	40
11	4	4	40
12	3	4	40
13	3	2	30
14	3	6	50
15	5	6	50
16	4	4	40
17	3	2	50
18	4	2	40
19	4	6	40
20	5	4	40

3. Results and Discussion

3.1. Characterization of Bio-Coagulants and Paint Wastewater Sample

The characterization results for the bio-coagulants—functional groups and proximate analysis—along with the wastewater sample before and after treatment are presented in Tables 2–4. Table 2 summarizes the functional groups identified in PS and MOS bio-coagulants by FTIR analysis, with their proposed roles in coagulation-flocculation interpreted according to established mechanisms reported in the literature [4,7]. This analysis revealed key functional groups—amines (N-H), carbonyls (C=O), alcohols (C-O), and alkyl/alkane groups (C-H)—that are associated with proteins and polysaccharides and that may promote coagulation primarily through charge neutralization and particle bridging, thereby supporting floc formation and improving TDS removal [3,4]. Together, these results point to both PS and MOS as suitable, environmentally friendly, and sustainable options for treating industrial wastewater.

The proximate analysis results in Table 3 highlight the components that most influence bio-coagulant performance. *Moringa oleifera* seed (MOS) had a higher yield (30.52%) and a markedly higher protein content (37.5%) than avocado pear seed (PS), which had a yield of 25.63% and a protein content of 18.5%, whereas PS had a higher carbohydrate content (53.08% versus 44.63% for MOS). The high protein content of MOS enhances charge neutralization and thus strengthens floc formation, while the higher carbohydrate content of PS improves particle bridging and provides structural support during floc aggregation [4,7]—explaining why the two bio-coagulants differ in TDS removal efficiency.

2026, Vol. 2, Article ID. 2026.0028
https://doi.org/10.69709/SusProc.2026.188988

Table 4 shows that the untreated paint wastewater sample had an initial TDS concentration of 2524.43 mg/L. Post-treatment TDS values dropped considerably with both bio-coagulants, falling to 165.54 mg/L with PS and 100.13 mg/L with MOS, corresponding to removal efficiencies of approximately 93.44% and 96.03%, respectively. This confirms that both bio-coagulants effectively promoted flocculation and sedimentation, improving overall water quality; the superior performance of MOS, in particular, can be linked to its higher protein content and favorable functional groups, which enhance charge neutralization and floc formation and thereby improve dissolved solids removal [4]. These pre- and post-treatment measurements represent the wastewater characterization experiments which are different from the experimental responses generated subsequently through the RSM design and the independent validation experiments.

3.2. RSM and ANN Results of TDS Removal Using Avocado Pear and *Moringa oleifera* Seed Bio-Coagulants

Table 5 present the combined RSM and ANN results for TDS removal using avocado pear and *Moringa oleifera* seed bio-coagulants. Both materials performed effectively across the design space, with removal efficiencies ranging from 57–93% for avocado pear seed (PS) and 61–97% for *Moringa oleifera* seed (MOS); in both cases, the highest and most consistent removal efficiencies occurred at the center-point conditions of 4 mg/L dose, pH 4-, and 40-min settling time, pointing to a consistent and effective coagulation range. Predicted values for PS agreed well with the experimental results, with only minor discrepancies at the extreme factorial points—an unsurprising outcome, since particle destabilization and floc formation can vary considerably under very high or low pH and dosage levels [19]. ANN predictions for MOS, by contrast, tracked the experimental data even more closely, underscoring the stronger predictive capability of the machine learning approach. Overall, these results indicate that both bio-coagulants are promising for TDS removal, with optimum performance concentrated at the middle values of the experimental parameters.

3.3. Model Fit Summary for TDS Removal

The model fit summary in Table 6 shows that the quadratic model provided the best fit for TDS removal efficiency with both coagulants: PS yielded an adjusted R^2 of 0.9874 and a predicted R^2 of 0.9416, while MOS yielded correspondingly high values of 0.9837 and 0.9194, indicating strong agreement between predicted and experimental responses. By comparison, the linear and two-factor interaction (2FI) models performed poorly, reflected in their low or negative predicted R^2 values, while the cubic models were aliased and could not be estimated or interpreted reliably [19].

Table 2: Characterization results of avocado Pear Seed (PS) and *Moringa oleifera* Seed (MOS) in terms of functional groups.

Bio-Coagulant	Functional Group	Class of Compound	Reported Role in Coagulation–Flocculation
PS	N-H stretch	bend Amines	Charge neutralization, floc formation
PS	C=O stretch	Aldehydes	Interaction with suspended particles
PS	C-O stretch	Alcohols	Bridging between particles
PS	C-H stretch	bend Alkanes Alkyls	Structural support in flocs
PS	C-F stretch	Alkyl halides	Surface activity, particle aggregation
MOS	N-H stretch	bend Amines	Charge neutralization, floc formation
MOS	C=O stretch	Esters	Interaction with suspended particles
MOS	C-O stretch	Alcohols Ethers	Bridging between particles
MOS	C-H stretch bend	Alkanes Alkyls	Aromatics Structural support in flocs
MOS	C-F stretch	Alkyl halides	Surface activity, particle aggregation

Table 3: Characterization results of PS and MOS in terms of proximate analysis.

Parameters	PS	MOS
Yield	25.63	30.52
Protein content (%)	18.5	37.5
Carbohydrate (%)	53.08	44.63

Table 4: Characterization results of paint wastewater pre- and post-treatment.

Parameter	PWW		
	Pre-Treatment	Post-Treatment with PS	Post-Treatment with MOS
Total solids (mg/L)	2599.67	171.87	106.46
Total suspended solids (mg/L)	75.24	6.33	6.33
Total dissolved solids (mg/L)	2524.43	165.54	100.13

Table 5: (**a**) Experimental and predicted TDS removal using avocado Pear Seed (PS) Bio-coagulant. (**b**) Experimental and predicted TDS removal using *Moringa oleifera* Seed (MOS) Bio-coagulant.

(a)

Run	Dosage (g)	pH	Time (min)	Experimental TDS Removal (%)	RSM Prediction (%)	ANN Prediction (%)
1	4	4	40	93.16	93.53	93.28
2	5	6	30	68.64	68.16	68.76
3	5	2	50	81.58	82.14	81.7
4	3	6	30	57.41	57.12	57.53
5	4	4	30	82.07	82.65	82.19
6	4	4	50	92.01	90.33	92.13
7	4	4	40	93.16	93.53	93.28
8	4	4	40	93.16	93.53	93.28
9	5	2	30	73.58	74.49	73.7
10	4	4	40	93.16	93.53	93.28
11	4	4	40	93.16	93.53	93.28
12	3	4	40	81.71	82.59	81.83
13	3	2	30	74.4	73.68	74.52
14	3	6	50	65.46	64.83	65.58
15	5	6	50	78.87	79.87	78.99
16	4	4	40	93.16	93.53	93.28
17	3	2	50	76.57	77.33	76.69
18	4	2	40	92.44	90.93	92.56
19	4	6	40	81.11	81.51	81.23
20	5	4	40	92.5	90.51	92.62

(b)

Run	Dosage (g)	pH	Time (min)	Experimental TDS Removal (%)	RSM Prediction (%)	ANN Prediction (%)
1	4	4	40	96.75	97.25	96.75
2	5	6	30	72.29	71.29	72.29
3	5	2	50	85.23	85.68	85.23
4	3	6	30	61.04	60.97	61.04
5	4	4	30	85.72	86.26	85.72
6	4	4	50	95.68	93.65	95.68
7	4	4	40	96.75	97.25	96.75
8	4	4	40	96.75	97.25	96.75
9	5	2	30	77.22	78.32	77.22
10	4	4	40	96.75	97.25	96.75
11	4	4	40	96.75	97.25	96.75
12	3	4	40	85.36	85.35	85.36
13	3	2	30	75.54	74.98	75.54
14	3	6	50	69.11	68.39	69.11
15	5	6	50	82.52	83.46	82.52
16	4	4	40	96.75	97.25	96.75
17	3	2	50	76.22	77.59	76.22
18	4	2	40	96.09	93.74	96.09
19	4	6	40	84.76	85.62	84.76
20	5	4	40	96.03	94.55	96.03

2026, Vol. 2, Article ID. 2026.0028
https://doi.org/10.69709/SusProc.2026.188988

Table 6: Model fit summary for TDS removal using avocado Pear Seed (PS) and *Moringa oleifera* Seed (MOS).

Bio-Coagulant	Model Type	Sequential *p*-Value	Lack of Fit *p*-Value	Adjusted R^2	Predicted R^2	Recommendation
PS	Linear	0.2283	-	0.0868	−0.4213	
PS	2FI	0.9105	-	−0.0800	−4.8177	
PS	Quadratic	<0.0001	-	0.9874	0.9416	Suggested
PS	Cubic	0.0221	-	0.9961	−0.5144	Aliased
MOS	Linear	0.2619	-	0.0682	−0.4491	
MOS	2FI	0.9514	-	−0.1178	−5.0586	
MOS	Quadratic	<0.0001	-	0.9837	0.9194	Suggested
MOS	Cubic	0.0513	-	0.9932	−1.6385	Aliased

3.4. Analysis of Variance for TDS Removal

The analysis of variance (ANOVA) results, presented in Table 7, further confirm the suitability of the quadratic model for both bio-coagulants. In both tables, the linear (A, B, C), interactive (AB, AC, BC), and quadratic (A^2, B^2, C^2) terms were all statistically significant ($p < 0.05$) [19], showing that TDS removal depends on both individual factors and their interactions. The relatively high F-values for dosage, pH, and settling time in both models likewise confirm that these process factors significantly shape the coagulation-flocculation process. The predicted R^2 values of 0.9416 and 0.9194 for PS and MOS, respectively, align reasonably well with their adjusted R^2 values of 0.9874 and 0.9837, with differences under 0.1 in each case, while Adequate Precision ratios of 41.9060 (PS) and 35.9382 (MOS)—both well above the desirable threshold of 4—indicate adequate signal-to-noise ratios for navigating the design space [19,27]. Taken together, the Model Fit Summary (Section 3.3) and these ANOVA results confirm that the quadratic RSM model fits the data well and captures both the nonlinear and interaction effects governing TDS removal, providing a reliable basis for numerical optimization, response surface generation, and comparison against the ANN models.

Table 7: (**a**) ANOVA for TDS removal using avocado Pear Seed (PS). (**b**) ANOVA for TDS removal using *Moringa oleifera* Seed (MOS).

(a)

Source	Sum of Squares	Df	Mean Square	F-Value	*p*-Value	
Model	2262.37	9	251.37	166.54	<0.0001	Significant
A-Dosage	156.97	1	156.97	104.00	<0.0001	
B-pH	221.65	1	221.65	146.85	<0.0001	
C-Time	147.38	1	147.38	97.64	<0.0001	
AB	52.28	1	52.28	34.63	0.0002	
AC	8.02	1	8.02	5.31	0.0439	
BC	8.22	1	8.22	5.45	0.0418	
A^2	133.88	1	133.88	88.70	<0.0001	
B^2	146.84	1	146.84	97.29	<0.0001	
C^2	136.38	1	136.38	90.36	<0.0001	
Residual	15.09	10	1.51			
Lack of Fit	15.09	5	3.02			
Pure Error	0.0000	5	0.0000			
Cor Total	2277.46	19				
Std. Dev.	1.23		R^2		0.9934	
Mean	82.87		Adjusted R^2		0.9874	
C.V. %	1.48		Predicted R^2		0.9416	
			Adeq Precision		41.9060	

Table 7: *Cont.*

(b)						
Source	**Sum of Squares**	**Df**	**Mean Square**	**F-Value**	***p*-Value**	
Model	2361.67	9	262.41	128.73	<0.0001	Significant
A-Dosage	211.78	1	211.78	103.90	<0.0001	
B-pH	164.67	1	164.67	80.79	<0.0001	
C-Time	136.53	1	136.53	66.98	<0.0001	
AB	24.40	1	24.40	11.97	0.0061	
AC	11.26	1	11.26	5.52	0.0406	
BC	11.54	1	11.54	5.66	0.0386	
A^2	146.55	1	146.55	71.89	<0.0001	
B^2	157.59	1	157.59	77.31	<0.0001	
C^2	146.35	1	146.35	71.80	<0.0001	
Residual	20.38	10	2.04			
Lack of Fit	20.38	5	4.08			
Pure Error	0.0000	5	0.0000			
Cor Total	2382.05	19				
Std. Dev.	1.43		R^2		0.9914	
Mean	86.17		Adjusted R^2		0.9837	
C.V. %	1.66		Predicted R^2		0.9194	
			Adeq Precision		35.9382	

3.5. Mathematical Model Equations for TDS Removal Using Avocado Pear Seed (PS) and *Moringa oleifera* Seed (MOS)

Building on the significant model terms identified through the quadratic ANOVA analysis (Section 3.4), mathematical models were developed relating dosage (A), pH (B), and settling time (C) to the TDS removal efficiencies of PS (TDS_{PS}) and MOS (TDS_{MOS}). Equations (5) and (6) present the fitted second-order polynomials—including linear, interaction, and quadratic terms—generated from the CCD experimental design, serving as predictive tools for estimating TDS removal within the studied factor ranges; both final empirical models are expressed here in terms of coded factors.

$$\begin{aligned} TDS_{PS} &= 93.53 + 3.96A - 4.71B + 3.84C + 2.56AB \\ &+1.00AC + 1.01BC - 6.98A^2 - 7.31B^2 - 7.04C^2 \end{aligned} \tag{5}$$

$$\begin{aligned} TDS_{MOS} &= 97.25 + 4.60A - 4.06B + 3.69C + 1.75AB \\ &+1.19AC + 1.20BC - 7.30A^2 - 7.57B^2 - 7.29C^2 \end{aligned} \tag{6}$$

3.6. Graphical Analysis of TDS Removal Using Avocado Pear Seed and *Moringa oleifera* Seed

3.6.1. Predicted vs. Experimental Plots

Figure 1 present the predicted versus experimental TDS removal values for PS and MOS, respectively. In both cases, the data points cluster closely around the 45° line representing perfect agreement between predicted and experimental values, indicating a close fit between the RSM predictions and observed responses, with the resulting linear plots clustering closely along the lines of best fit—evidence that the generated models can adequately predict the TDS removal efficiency of both PS and MOS [27].

3.6.2. 3D Response Surface Plots for TDS Removal

A 3D response surface was generated to estimate how combinations of the independent variables affect TDS removal efficiency for both coagulants; the resulting plots appear in Figure 2. For both coagulants, increasing dosage improved TDS removal, whereas pH and settling time each showed nonlinear effects. Figure 2a,d show that pH has a more prominent effect at moderate to high dosage levels, pointing to a specific pH range where TDS removal is most effective, while Figure 2b,e show that longer settling times improved removal efficiency, particularly in combination with higher dosages. Overall, the response surfaces exhibit distinct maxima rather than flat trends, confirming that specific combinations of these variables yield optimal TDS removal.

3.6.3. Artificial Neural Network Regression Plots

Figure 3 present the artificial neural network (ANN) regression plots for TDS removal from paint wastewater, based on data divided into training (70%), validation (20%), and testing (10%) subsets. In both figures, the

2026, Vol. 2, Article ID. 2026.0028
https://doi.org/10.69709/SusProc.2026.188988

training regression plots show near-perfect correlation (R = 1) between predicted outputs and experimental targets, the validation regressions show high correlation coefficients (R ≈ 0.969 in Figure 3a and R ≈ 0.9698 in Figure 3b) with data points closely distributed around the best-fit line, again reach R=1, although the test subset contains only two observations and does not conclusively demonstrate model generalization. Combined with the very low RMSE and SEP values reported in Section 3.7, these results further confirm the ANN model's superior predictive performance over RSM in capturing nonlinear interactions [19].

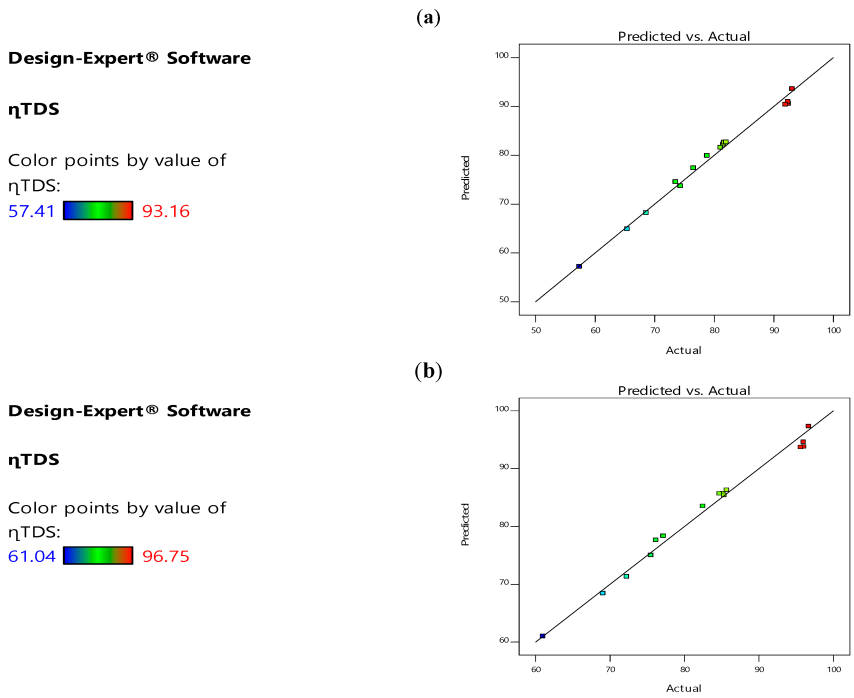

Figure 1: Predicted vs. experimental TDS removal: (**a**) Using avocado Pear Seed (PS) and (**b**) using *Moringa oleifera* Seed (MOS) Bio-Coagulants.

3.7. Predictive Performance Metrics (R^2, RMSE, SEP) of RSM and ANN for Avocado Pear Seed and *Moringa oleifera* Seed

Table 8 summarizes the predictive performance of the RSM and ANN models for TDS removal using PS and MOS bio-coagulants. The reported root mean square error (RMSE), standard error of prediction (SEP), and coefficient of determination (R^2) are a quantitative basis for evaluating the accuracy of each modeling approach.

3.8. Comparative RSM and ANN Modeling

The predictive performance of the RSM and ANN models, developed using Design-Expert and MATLAB respectively, was compared using RMSE, SEP, and the coefficient of determination (R^2). R^2 reflects the percentage of variation in TDS removal efficiency explained by the model, with values close to unity indicating strong agreement between experimental and predicted results [18,19,27]; RMSE and SEP were also examined, however, Since R^2 alone does not fully capture model accuracy, and lower values of both indicate reduced prediction error and greater model reliability [18,21]. For PS, the ANN model achieved an R^2 of 0.9998 against 0.990407 for RSM, while RMSE and SEP fell from 0.86902 and 1.048711 to 0.12 and 0.144813, respectively. For MOS, the ANN R^2 similarly approached unity (1.0000), with RMSE and SEP dropping sharply from 1.009331 and 1.171387 under RSM to 5.3×10^{-5} and 6.15×10^{-5}. This improved accuracy suggests within the present dataset that the ANN model captured the nonlinear relationships among dosage, pH, settling time, and TDS removal efficiency more closely than the quadratic RSM model, suggesting that the coagulation-flocculation process involves complex nonlinear relationships not fully represented by the second-order polynomial structure of the RSM model [16]. Nevertheless, the exceptionally high R^2 and extremely

low prediction errors obtained for MOS warrant caution, since the relatively small experimental dataset available for model development may have contributed to this unusually strong predictive performance. While these results demonstrate ANN's strong predictive capability for this system, future studies should therefore employ larger datasets and cross-validation approaches to further assess model generalization and robustness across broader operating conditions.

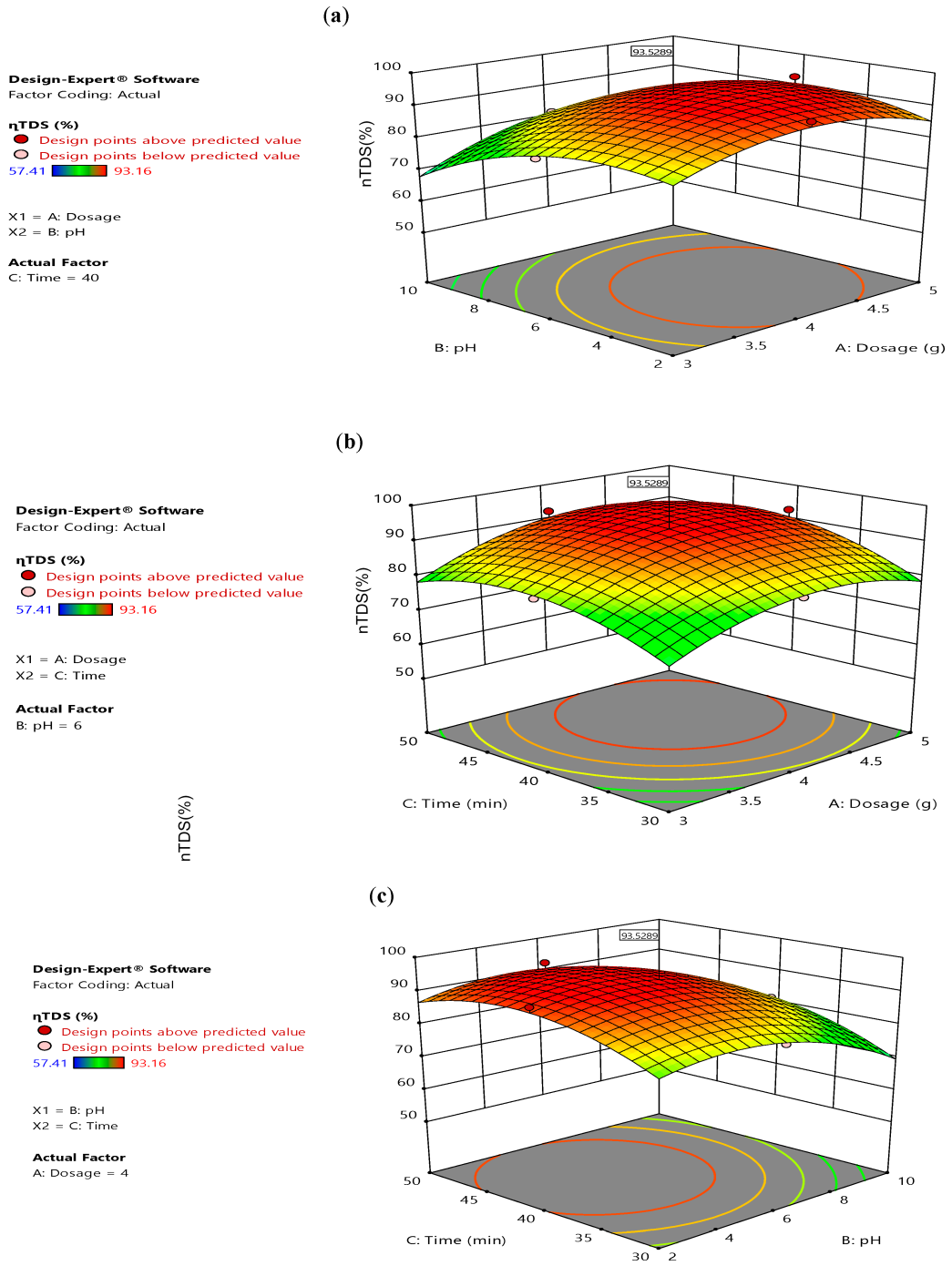

Figure 2: *Cont.*

2026, Vol. 2, Article ID. 2026.0028
https://doi.org/10.69709/SusProc.2026.188988

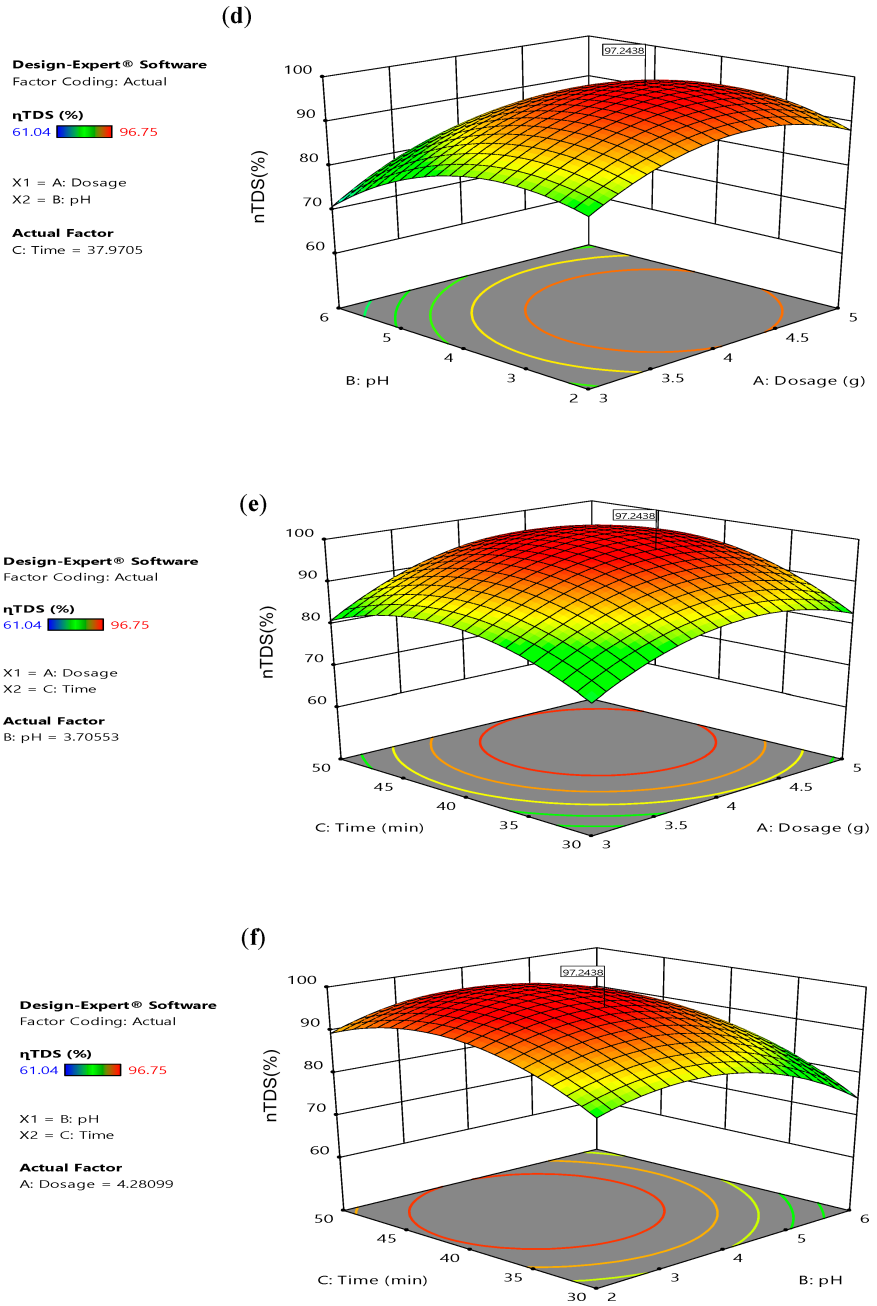

Figure 2: Response surface plots showing the interactive effects of dosage, pH, and treatment time on TDS removal: (**a**) dosage–pH interaction at fixed treatment time; (**b**) dosage–treatment time interaction at fixed pH; (**c**) pH–treatment time interaction at fixed dosage, for avocado pear seed (PS) bio-coagulant; and (**d**) dosage–pH interaction at fixed treatment time; (**e**) dosage–treatment time interaction at fixed pH; (**f**) pH–treatment time interaction at fixed dosage, for *Moringa oleifera* seed (MOS) bio-coagulant.

Table 8: Predictive performance metrics (R^2, RMSE, SEP) of RSM and ANN for avocado Pear Seed (PS) and *Moringa oleifera* Seed (MOS).

Bio-Coagulant	Model	RMSE	SEP	R^2
PS	RSM	0.86902	1.048711	0.990407
PS	ANN	0.12	0.144813	0.9998
MOS	RSM	1.009331	1.171387	0.987555
MOS	ANN	5.3×10^{-5}	6.15×10^{-5}	1.0000

3.9. Optimum Parameters for TDS Removal from Paint Wastewater Using Avocado Pear and *Moringa oleifera* Seed Bio--Coagulants

Table 9 presents the optimum operating conditions identified through numerical optimization, together with their corresponding desirability values. For PS, the optimization predicted a maximum TDS removal of 93.53% at a dosage of 4.00 (g), pH 6.00, and a settling time of 40 min, with a desirability of 0.99. Although the highest experimental removal efficiency occurred at the center-point condition of pH 4, dosage 4 (g), and settling time 40 min, the RSM optimization identified pH 6 as the mathematical optimum; the small gap between the experimental maximum (93.16%) and the optimized prediction (93.53%) suggests that PS removal efficiency remained relatively stable across the pH range studied, with several operating conditions capable of achieving similarly high removal [18,19]. For MOS, the optimal conditions were estimated at a dosage of 4.28 g, pH 3.71, and a settling time of 37.97 min, yielding an RSM optimized predicted TDS removal efficiency of 97.24% and a desirability of 1.00. These optimal MOS conditions sat close to the center of the design space but shifted slightly toward acidic pH and shorter settling time, implying that MOS can achieve strong treatment performance under mildly acidic conditions without requiring extended settling periods. The high desirability values obtained for both bio-coagulants confirm that the optimized solutions effectively meet the objective of maximizing TDS removal [18,19].

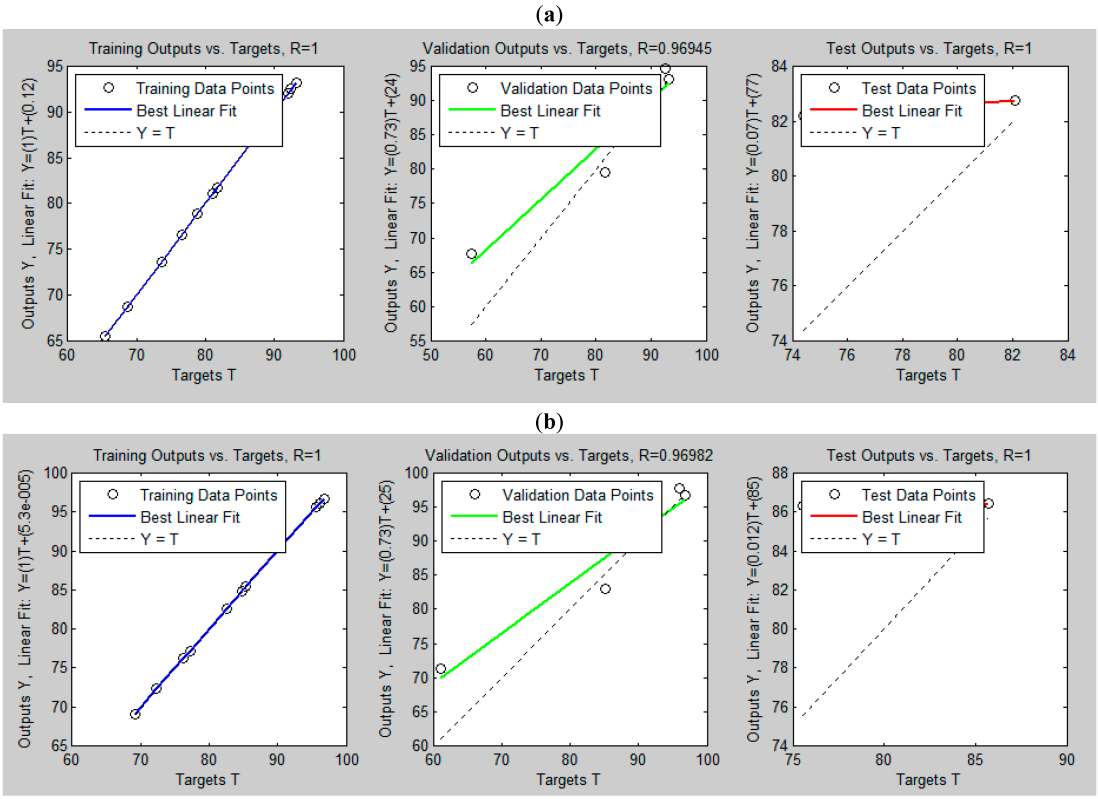

Figure 3: ANN regression of TDS removal from paint wastewater: (**a**) Using avocado Pear Seed (PS) and (**b**) using *Moringa oleifera* Seed (MOS) Bio-Coagulants.

Table 9: Optimized conditions for TDS removal from paint wastewater using Avocado Pear Seed (PS) and *Moringa oleifera* Seed (MOS) Bio-Coagulants.

Bio-Coagulant	Optimum Dosage (g)	Optimum pH	Optimum Time (min)	Optimum TDS (%)	Desirability
PS	4.00	6.00	40.00	93.53	0.99
MOS	4.28	3.71	37.97	97.24	1.00

2026, Vol. 2, Article ID. 2026.0028
https://doi.org/10.69709/SusProc.2026.188988

3.10. Validation of Optimal Parameter Results

Validation studies were conducted using the identified optimum process parameters for both PS and MOS bio-coagulants to confirm the reliability of the developed models and the predicted optimum operating conditions. Experiments were run in triplicate under these optimal conditions, and the resulting mean values were compared against the model predictions. As shown in Table 10, the average independent experimental validation TDS removal efficiencies were 92.87 ± 0.65% for PS and 96.49 ± 0.39% for MOS, closely matching the RSM predicted removals of 93.53% and 97.24%, respectively, with percentage deviations of only 0.71% and 0.78%—confirming that the models predict treatment performance effectively. The low standard deviations further indicate good repeatability of the coagulation-flocculation process under optimal conditions, and the combination of low experimental variability with sub-1% prediction deviations indicates close agreement between the validation results and predictions of the optimized parameters for TDS removal from paint wastewater, consistent with validation criteria applied in similar optimization studies [18,19,27].

Table 10: Experimental validation of optimized conditions for TDS removal from paint wastewater using avocado Pear Seed (PS) and *Moringa oleifera* Seed (MOS) Bio-Coagulants.

Bio-Coagulant	Optimum Dosage (g)	Optimum pH	Optimum Time (min)	Experimental TDS Removal (%)(Mean ± SD)	Predicted TDS Removal (%)	Percentage Deviation (%)
PS	4.00	4.00	40.00	92.87 ± 0.65	93.53	0.71
MOS	4.28	3.71	37.97	96.49 ± 0.39	97.24	0.78

3.11. Practical Implications, Techno-Economic Considerations, Sustainability and Future Scale-Up Perspectives

Avocado pear and *Moringa oleifera* seeds are abundant agricultural materials in many tropical countries, often discarded as underutilized biomass waste. Using these bio-coagulants could therefore reduce dependence on commercially produced chemical coagulants, lowering treatment costs while adding value to agricultural waste streams. Although a full techno-economic analysis fell outside the scope of this study, the use of locally available biomass suggests strong economic potential for decentralized, small-scale wastewater treatment systems, consistent with similar studies highlighting the economic attractiveness of plant-derived treatment materials owing to their low acquisition costs, renewability, and reduced environmental burden relative to synthetic treatment chemicals [11–13]. Beyond its economic relevance, this study directly supports several United Nations Sustainable Development Goals (SDGs): effective paint wastewater treatment contributes to SDG 6 (Clean Water and Sanitation) by improving water quality management [11,12]; the use of plant-based waste materials as bio-coagulants aligns with SDG 12 (Responsible Consumption and Production) through resource recovery and waste valorization [28]; replacing conventional chemical coagulants with biodegradable alternatives supports SDG 13 (Climate Action) by reducing the environmental impact of chemical production and disposal [16]; and data-driven optimization methods such as RSM and ANN advance SDG 9 (Industry, Innovation and Infrastructure) by encouraging new, sustainable wastewater treatment solutions [9,12]. This data-driven modeling approach could offer a broader framework for process design, operational control, and performance prediction, supporting future scale-up efforts—though pilot-scale studies will still be needed to evaluate process stability under continuous flow and varying wastewater compositions. Several limitations nonetheless remain: this study did not examine the potential for bio-coagulant regeneration or reuse after treatment, nor the properties or management of the resulting sludge. Future work should therefore evaluate coagulant reuse cycles, treatment efficiency after repeated use, sludge formation rates, and the potential for sludge valorization as a soil amendment or other beneficial application.

4. Conclusions

In this work, bio-coagulants made from avocado pear seed (PS) and *Moringa oleifera* seed (MOS) were used effectively as sustainable coagulants for TDS removal from paint wastewater, achieving RSM predicted removal efficiencies of 93.53% for PS and 97.24% for MOS. This strong performance was linked to the presence of proteins and polysaccharides that support charge neutralization and

floc formation. Response Surface Methodology was further applied to identify the optimal dosage, settling time, and pH, and the resulting optimal conditions were validated with percentage deviations below 1%, indicating that both the model predictions and the identified conditions are reliable and practical. The comparative analysis of the two modeling techniques showed that ANN consistently produced more accurate predictions than RSM, demonstrating the value of combining standard statistical methods with machine learning in the design and optimization of wastewater treatment processes that employ plant-based coagulants.

5. Limitations and Future Research

One limitation of this study is the relatively small dataset used to develop the ANN model, a consequence of the experimental design matrix. Although the resulting ANN models achieved high predictive accuracy, future studies should draw on larger experimental datasets and more advanced validation procedures—such as k-fold cross-validation and external validation datasets—to further test model robustness and generalizability. Doing so would strengthen confidence in applying ANN models to large-scale industrial wastewater treatment optimization.

List of Abbreviations

ANN	Artificial Neural Network
ANOVA	Analysis of Variance
CCD	Central Composite design
C.V. %	Coefficient of Variation
EDTA	Ethylenediaminetetraacetic Acid
2FI	Two-Factor Interaction
FTIR	Fourier Transform Infrared Spectroscopy
MOS	*Moringa oleifera* Seed
MSE	Mean Square Error
PS	Avocado Pear Seed
PWW	Paint Wastewater
RMSE	Root Mean Square Error
R^2	Coefficient of Determination
RSM	Response Surface Methodology
SD	Standard Deviation
SDGs	Sustainable Development Goals
SEP	Standard Error of Prediction
TDS	Total Dissolved Solids

Author Contributions

Conceptualization, O.S.N., B.C.U., and C.O.A.; Methodology, O.S.N. and B.C.U.; Software, formal analysis, and data curation, C.O.A. and O.S.N.; Validation and supervision, O.S.N. and B.C.U.; Investigation, writing—original draft preparation, writing—review and editing, and visualization, C.O.A.; Resources and project administration, O.S.N. All authors have read and agreed to the published version of the manuscript.

Availability of Data and Materials

Data supporting the findings of this study are available from the corresponding author upon reasonable request.

Conflicts of Interest

The authors declare no conflicts of interest.

Funding

The study did not receive any external funding and was conducted using only institutional resources.

Acknowledgments

The authors acknowledge the Department of Chemical Engineering, Enugu State University of Science and Technology (ESUT), Enugu, Nigeria, for providing laboratory support for this study, and also thank the management of Legacy Paints Limited, Industrial Layout, Emene, Enugu State, Nigeria, for granting access to the paint wastewater samples used in this research.

AI Declaration

The authors confirm that no AI tools were used to generate or rephrase any part of the manuscript text. All aspects of the study---including research design, data collection, data analysis, interpretation of findings, and manuscript preparation and revision---were carried out solely by the authors. The authors take full responsibility for the accuracy, originality, integrity, and scientific content of the manuscript.

References

[1] Nair, K.S; Manu, B.; Azhoni, A. Sustainable Treatment of Paint Industry Wastewater: Current Techniques and Challenges. *J. Environ. Manag.* **2021**, *296*, 113105. [CrossRef]

[2] Yadav, D.; Dutta, J. Advancing Environmental Sustainability: Recent Trends and Developments in Treatment Methods for Paint Industry Wastewater. *J. Water Process Eng.* **2024**, *61*, 105290. [CrossRef]

[3] Koul, B.; Bhat, N.; Abubakar, M.; Mishra, M.; Arukha, A.P.; Yadav, D. Application of Natural Coagulants in Water Treatment: A Sustainable Alternative to Chemicals. *Water* **2022**, *14*, 3751. [CrossRef]

[4] Elsergany, M. The Potential Use of *Moringa peregrina* Seeds and Seed Extract as a Bio-Coagulant

for Water Purification. *Water* **2023**, *15*(15), 2804. [CrossRef]

[5] Santos, A.L.A.; Araújo, T.D.; Michelan, D.C.D.G.S. Toxicity of Sludge from Water Treatment Using Natural Coagulants/Floculants. *J. Water Process Eng.* **2025**, *77*, 108644. [CrossRef]

[6] Wang, N.; Li, X.; Yang, Y.; Shang, Y.; Zhuang, X.; Li, H.; Zhou, Z. Combined Process of Visible Light Irradiation Photocatalysis-Coagulation Enhances Natural Organic Matter Removal: Optimization of Influencing Factors and Mechanism. *Chem. Eng. J.* **2019**, *374*, 748–759. [CrossRef]

[7] Fu, S.; Li, D.; Fu, K.; Zhu, Y.; Yang, S.; Zhang, X.; Zhang, J. Towards a High-Rate Operation of Contact Stabilization Process: Challenges of Flocculation and Floc Stability. *J. Environ. Manag.* **2024**, *370*, 123014. [CrossRef] [PubMed]

[8] Meftah, K.; Meftah, S.; Lamkhanter, H.; Bouzid, T.; Rezzak, Y.; Touil, S.; Abid, A. Extraction and Optimization of *Austrocylindropuntia subulata* Powder as a Novel Green Coagulant. *Desalin. Water Treat.* **2024**, *318*, 100339. [CrossRef]

[9] Meftah, K.; Meftah, S.; Ballou, I.; Bouzid, T.; Touil, S.; Abid, A. Impact of Storage Conditions of *Opuntia ficus-indica* Pieces on Plant Quality, Powder Composition, and Extracted Bioflocculant Efficiency. *Environ. Sci. Pollut. Res.* **2025**, *32*, 26840–26857. [CrossRef] [PubMed]

[10] Rosa, D.; Cifaldi, D.; Di Palma, L. Boron Removal from Wastewater via Coordinative Adsorption Assisted by Fenton-Induced Oxoprecipitation/Flocculation. *Chem. Eng. J.* **2024**, *498*, 155572. [CrossRef]

[11] Meftah, S.; Meftah, K.; Drissi, M.; Radah, I.; Malous, K.; Amahrous, A.; Chahid, A.; Tamri, T.; Rayyad, A.; Darkaoui, B.; et al. Heavy Metal Polluted Water: Effects and Sustainable Treatment Solutions Using Bio-Adsorbents Aligned with the SDGs. *Discov. Sustain.* **2025**, *6*(1), 137. [CrossRef]

[12] Meftah, S.; Meftah, K.; Babassa, N.; Malous, K.; Drissi, M.; Amahrous, A.; Jabri, N.; Fathi, J.; Aguerchi, K.; Laababid, Y.; et al. The Versatility and Effectiveness of Bio-Adsorbents in the Removal of Chemical Pollutants from Water: Adsorption Mechanisms, Optimization by ANN and RSM, SWOT Analysis, and Contribution to the 3rd and 6th Sustainable Development Goals. *Discov. Sustain.* **2025**, *6*(1), 971. [CrossRef]

[13] Meftah, S.; Meftah, K.; Lamkhanter, H.; Taib, M.; Amahrous, A.; Assadi, F.; Oukani, E.H.; Bouyazza, L. The Main Types of Derivatives of Plant Matter and Agricultural Waste Used as Bio-Adsorbents for the Removal of Heavy Metals and Dyes: A Review. *Egypt. J. Chem.* **2024**, *67*(9), 185–207. [CrossRef]

[14] Ayat, A.; Arris, S.; Abbaz, A.; Bencheikh-Lehocine, M.; Meniai, A.H. Application of Response Surface Methodology for Modelling and Optimization of a Bio Coagulation Process (Sewage Wastewater Treatment Plant). *Environ. Manag.* **2021**, *67*, 489–497. [CrossRef]

[15] Jasni, A.B.; Kamyab, H.; Chelliapan, S.; Arumugam, N.; Krishnan, S.; Din, M.F.M. Treatment of Wastewater Using Response Surface Methodology: A Brief Review. *Chem. Eng. Trans.* **2020**, *78*, 535–540. [CrossRef]

[16] Chen, Y.; Song, L.; Liu, Y.; Yang, L.; Li, D. A Review of the Artificial Neural Network Models for Water Quality Prediction. *Appl. Sci.* **2020**, *10*, 5776. [CrossRef]

[17] Chandanshive, V.; Shanbhag, A. Application of Artificial Neural Network in Environmental Engineering-A State-of-the-Art Review. *Int. J. Environ. Waste Manag.* **2024**, *33*, 499–510. [CrossRef]

[18] Han, K.; Wang, Y. A Review of Artificial Neural Network Techniques for Environmental Issues Prediction. *J. Therm. Anal. Calorim.* **2021**, *145*, 2191–2207. [CrossRef]

[19] Mohammed, N.; Palaniandy, P.; Shaik, F.; Mewada, H.; Balakrishnan, D. Comparative Studies of RSM Box-Behnken and ANN-Anfis Fuzzy Statistical Analysis for Seawater Biodegradability Using TiO_2 Photocatalyst. *Chemosphere* **2023**, *314*, 137665. [CrossRef]

[20] Zahmatkesh, S.; Karimian, M.; Chen, Z.; Ni, B.J. Combination of Coagulation and Adsorption Technologies for Advanced Wastewater Treatment for Potable Water Reuse: By ANN, NSGA-II, and RSM. *J. Environ. Manag.* **2024**, *349*, 119429. [CrossRef] [PubMed]

[21] Rasheed, A.A. Improving Prediction Efficiency by Revolutionary Machine Learning Models. *Mater. Today Proc.* **2023**, *81*, 577–583. [CrossRef]

[22] Ding, C.; Shen, L.; Liang, Q.; Li, L. Machine Learning in Flocculant Research and Application: Toward Smart and Sustainable Water Treatment. *Separations* **2025**, *12*(8), 203. [CrossRef]

[23] Meftah, S.; Meftah, K.; Ballou, I.; Amahrous, A.; Darkaoui, B.; Belcaid, A.; Taib, M.; Malous, K.; El-Hassan, O.; Bouyazza, L. Optimization of Indigo Carmine Dye Removal by a Novel H_3PO_4-Activated Carbon Derived from (*Quercus suber* L.) Leaves Using the RSM-BBD and ANN. *Environ. Sci. Pollut. Res.* **2025**, *32*, 26576–26601. [CrossRef] [PubMed]

[24] Babassa, N.; Anouar, M.; Msaad, A.; Meftah, S.; Amahrous, A.; Bannour, O.; Adnouss, O.; Kadmi, Y.; Anouar, A. Response Surface Modelling of Methylene Blue Adsorption onto *Ceratonia siliqua* Leaves. *J. Environ. Eng. Sci.* **2026**, 1–10. [CrossRef]

[25] Ezemagu, I.G.; Ejimofor, M.I.; Menkiti, M.C.; Nnaji, P.C.; Anadebe, V.C. Application of *Terebralia palustris* Shell Extract for Bio-Coagulation Treatment of Produced Water and Digestion of Generated Sludge into Enriched Biomethane. *J. Clean. Prod.* **2023**, *390*, 136063. [CrossRef]

[26] Ahsan, M.A.; Satter, F.; Siddique, M.A.B.; Akbor, M.A.; Ahmed, S.; Shajahan, M.; Khan, R. Chemical and Physicochemical Characterization of Effluents from the Tanning and Textile Industries in

Bangladesh with Multivariate Statistical Approach. *Environ. Monit. Assess.* **2019**, *191*, 575. [CrossRef]

[27] Azinta, C.O.; Mbah, G.O.; Onoh, M.I. Optimization and Process Modeling of Viscosity of Oil-Based Drilling Muds. *J. Hum. Earth Future* **2021**, *2*, 412–423. [CrossRef]

[28] Babassa, N.; Anouar, M.; Msaad, A.; Meftah, S.; Amahrous, A.; Bannour, O.; Elidrissi, Z.M.; El Ghmari, B.; Balegh, F.E.; Kadmi, Y.; et al. Valorisation of *Ceratonia siliqua* Leaves as an Efficient Green Biosorbent for Dye Removal. *J. Environ. Eng. Sci.* **2025**, 1–13. [CrossRef]

Disclaimer/Publisher's Note: The views expressed in this article are those of the author(s) and do not necessarily reflect the views of the publisher or editors. The publisher and editors assume no responsibility for any injury or damage resulting from the use of information contained herein.